*Progress In Electromagnetics Research M, Vol. 85, 145–154, 2019*

# Wind Turbine Clutter Suppression for Weather Radars by Improved Range-Doppler Domain Joint Interpolation in Low SNR Environments

**Xu Yao[1], Mingwei Shen[1, *], Di Wu[2], and Daiyin Zhu[2]**

**Abstract**—Due to the exponential growth of the number and scale of wind farms, wind turbine clutter has become the main factor that limits the detection performance of weather radar systems. As a consequence of the rapid rotation of wind turbine blades, conventional ground clutter filters are ineffective at removing wind turbine clutter (WTC). An improved range-Doppler joint interpolation for WTC suppression is proposed in this paper. The proposed algorithm firstly exploits the frequency-domain transformation technique to improve the signal-to-noise ratio (SNR), so that the interpolation algorithm can recover the weather signal in the case of low SNR. Then, the weather signals recovered by one-dimensional interpolation in range domain and Doppler domain are calculated, respectively, and the two-dimensional joint interpolation is performed based on two-dimensional weighted coefficients calculated via a least mean squares criterion. Theoretical analysis and simulation results show that the proposed algorithm effectively suppresses the wind turbine clutter and significantly reduces the bias in radial velocity estimation caused by WTC contamination in low SNR environments.

## 1. INTRODUCTION

The rising cost of oil and the threat of global warming have urged the seeking for replacement of fossil fuels. As a clean and renewable energy, more and more countries become interested in wind energy. In recent years, a large number of wind farms have been built, and many wind farms are under construction. According to the report of American Wind Energy Association, the United States has an installed wind capacity of 61327 MW, and there are over 13000 MW currently under construction. Although with all the benefits of wind power, it becomes apparent that the wind turbine would have a negative impact on nearby radar systems. The unwanted returns from wind turbines are known as wind turbine clutter (WTC) [1] on nearby radar systems. The impacts of wind turbines on different radar systems, such as air traffic control, air surveillance, and weather radars [2] are different. The focus of this paper is the mitigation of WTC on weather radars.

A typical wind turbine is composed of two identifiable parts: a tower and blades. The tower provides a constant zero velocity return that can be suppressed by conventional clutter filters [3]. Unlike the tower, due to the rotation of blades, the Doppler spectrum of returns from blades varies from scan to scan. This time-varying radar signature results in the failure of classic clutter filter techniques. So, removing the effect of the blade motion is much more problematic. WTC is sometimes similar to the weather signal in power and spectral content, which make them difficult to distinguish on plan-position-indicator (PPI) weather-radar images. If not mitigated, WTC can contaminate weather radar data and cause the deviation of spectral moment estimation of the weather signal, such as reflectivity, radial

*Received 7 July 2019, Accepted 19 September 2019, Scheduled 29 September 2019*

* Corresponding author: Mingwei Shen (smw_hhu1981@163.com).

[1] College of Computer and Information Engineering, Hohai University, Nanjing 211100, China. [2] Key Laboratory of Radar Imagine and Microwave Photonics & Ministry of Education, Nanjing University of Aeronautics and Astronautics, Nanjing 210016, China.

velocity, and spectral width, which will greatly affect the detection performance of weather radars and cause the false detection and tracking of weather targets. Therefore, clutter suppression of wind turbines has become a core problem of clutter suppression of weather radars.

Several approaches have been developed for the mitigation of WTC in weather radars, such as those based on spatial interpolation, including multiquadric interpolation [4], Lagrange interpolation, spline interpolation, statistical invariant interpolation (ISI), etc. These methods aim to utilize reflectivity and radial velocity of the weather signal from neighbouring non-contaminated radar volumes to interpolate the reflectivity and radial velocity of the weather signal in contaminated locations. These methods regard weather data as spatial data and only make use of the spatial continuity of weather data. However, weather data are typical spatial-temporal data. The direct application of the spatial interpolation algorithm to spatial-temporal process may lead to the loss of valuable information in time dimension and affect the interpolation accuracy. Moreover, the spatial interpolation algorithms mentioned above do not take into account the influence of noise. In the case of low SNR, the spatial interpolation algorithms mentioned above fail to recover the weather signal.

In this paper, frequency-domain transformation is exploited to improve the signal-to-noise ratio, which can overcome the problem that the spatial interpolation algorithm cannot recover the weather signal in the case of low SNR. In an effort to improve the interpolation performance, the proposed algorithm extends one-dimensional spatial interpolation to two-dimensional joint interpolation in range-Doppler domain. The proposed algorithm assumes that general locations of the WTC contamination are known, and exploits spatial and spectral characteristics of the weather signal to mitigate the WTC contamination while having minimal impact on uncontaminated locations.

A description of the weather radar model is given in Section 2. The proposed algorithm is presented in Section 3. Simulation results and performance analyses are discussed in Section 4. Finally, conclusions and future work are given in Section 5.

## 2. WEATHER RADAR SIGNAL MODEL

In weather radar systems, assume that the $l$th range bin contains both WTC and weather signal. The radar returns in the $n$th pulse of the $l$th range bin can be expressed as:

$$x_l(n) = w_l(n) + c_l(n) + s_l(n) + z_l(n), \quad n = 1, 2, ..., K \tag{1}$$

where $K$ is the pulse number, $w_l(n)$ the wind turbine clutter, $c_l(n)$ the ground clutter, $s_l(n)$ the weather signal, and $z_l(n)$ the noise.

The weather signal is formed by the coherent superposition of all the scattering returns [5] in the $l$th range bin, assuming that the weather target is moving with a constant radial velocity. The weather signal return in the $n$th pulse of the $l$th range bin is given by:

$$s_l(n) = \sum_{u=1}^{U} A_u e^{j(n-1)\omega_t}, \quad n = 1, 2, ..., K \tag{2}$$

where $U$ is the total number of scattering points of weather targets in the $l$th range bin, and $A_u$ is the amplitude of the weather target particle $u$, which is determined by the radar equation. $\omega_t$ is the time domain angular frequency and can be written as:

$$\omega_t = \frac{4\pi v_u}{\lambda f_r} \tag{3}$$

where $v_u$ is the radial velocity of the weather target particle $u$, $\lambda$ the radar wavelength, and $f_r$ the pulse repetition frequency.

A wind turbine consists of two major scattering components, namely, a tower and blades. We study the spectral and temporal characteristics of WTC in detail [6–8]. The tower generates a constant zero velocity return that is easily mitigated by the conventional clutter filters. Unfortunately, the radar returns from blades are classified as time-varying clutter, and conventional clutter filters are ineffective at mitigating the time-varying WTC [9, 10] while preserving weather returns. The micro-Doppler signature of the wind turbine creates Doppler frequency shifts that can be spread across the Doppler spectrum. As a result, the spectrum of the wind turbine is wide. In addition, the WTC is similar to the weather

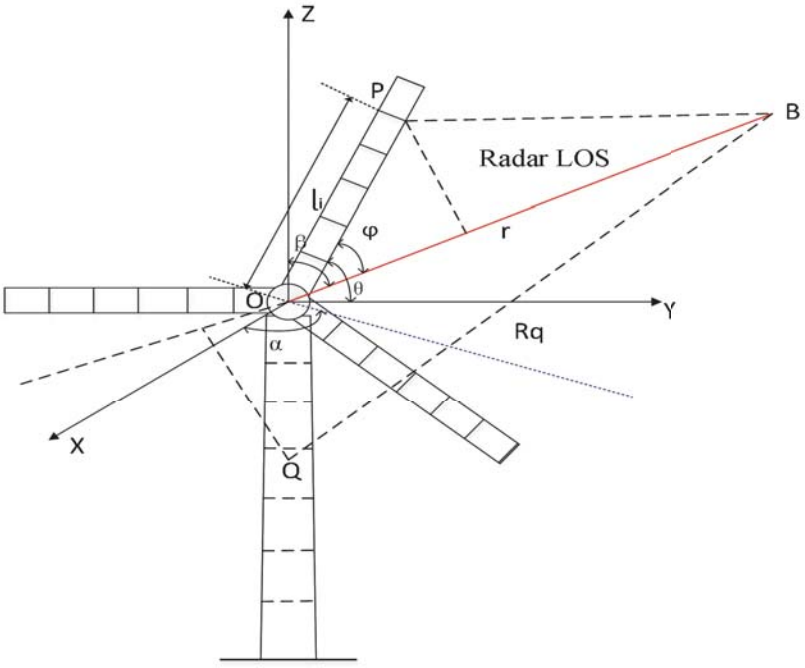


**Figure 1.** Relationship between the wind turbine and radar.

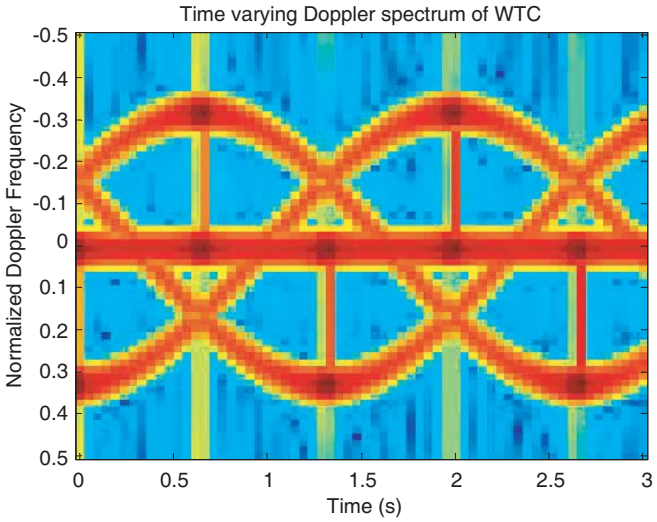


**Figure 2.** Time varying Doppler spectrum of WTC.

signal in power. Because of these two characteristics of WTC, the weather signal is often submerged in the Doppler spectrum of WTC. The relationship between the wind turbine and radar is shown in Fig. 1. The time varying Doppler spectrum of WTC is shown in Fig. 2.

## 3. WIND TURBINE CLUTTER MITIGATION

Typically, several conventional clutter-filtering techniques, such as finite impulse response (FIR) filters and Gaussian model adaptive processing (GMAP) are ineffective at removing the WTC while simultaneously preserving most of the weather signal. Due to the wide spectrum characteristics of wind turbine clutter, the weather signal is usually submerged in it, causing conventional methods to

fail in isolating the weather signal. Nuss and Titley [11] make use of multiquadric interpolation to recover the weather signal and attempt to mask the impact of WTC. The interpolation scheme has achieved some satisfactory results, but there are still some drawbacks. The multiquadric interpolation is one-dimensional spatial interpolation, while weather data are typical spatial-temporal data. The use of multiquadric interpolation to recover the weather signal will lose the information of time dimension, affecting the interpolation accuracy. Moreover, because of the influence of noise, the multiquadric interpolation fails to recover the weather signal in the case of low SNR.

### 3.1. Frequency-Domain Transformation

In practice, the accuracy of interpolation is greatly affected by SNR. In the case of low SNR, the interpolation performance of conventional multiquadric interpolation is significantly degraded. The conventional multiquadric interpolation is realized in time domain. In this paper, the radar return is first converted from time domain to frequency domain, and the SNR is improved by frequency-domain transformation. The frequency domain signal is expressed as follows:

$$X(k) = \sum_{n=1}^{K} x(n) e^{-j\frac{2\pi}{K}(n-1)k}, \quad k = 1, 2, ..., K \tag{4}$$

where $x(n)$ is the radar return, and $X(k)$ is its corresponding frequency domain expression.

After the above operation, the SNR is increased by $K$ times [12], avoiding the influence of noise on interpolation accuracy.

### 3.2. Improved Multiquadric Interpolation

Multiquadric interpolation was first proposed by Hardy [13] as a means of creating a regularly spaced grid from irregularly spaced topographical data. Franke [14] explores several global interpolation techniques and ranks the multiquadric method among the highest. Nuss and Titley make use of multiquadric interpolation with weather data and find that it outperforms both the Cressman and Barnes techniques. The multiquadric interpolation mentioned above is realized in time domain. In order to recover the weather signal in the case of low SNR, an improved multiquadric interpolation — frequency domain multiquadric interpolation is proposed in this paper.

Frequency domain multiquadric interpolation is the global interpolation technique that uses radial basis functions to approximate missing data. Assuming that the range bin number contaminated by WTC is $l$, the weather signal recovered by frequency domain multiquadric interpolation is given by:

$$\hat{X}_l(k) = \sum_{i=1}^{N} \alpha_i(k) Q(R_l - R_i) \tag{5}$$

and $Q(R_l - R_i)$ is a radial basis function defined as:

$$Q(R_l - R_i) = \left( \frac{\|R_l - R_i\|^2}{b^2} + 1.0 \right)^{\frac{1}{2}} \tag{6}$$

where $\hat{X}_l(k)$ is the recovered weather signal in the $k$th pulse of the $l$th range bin, $R_l$ the range of the $l$th range bin, $R_i$ the range of the $i$th range bin and $b$is a user-defined constant, $\alpha_i(k)$ the weighted factor in the $k$th pulse of the $i$th range bin, $N$ the total number of range bins selected, and $\|\cdot\|$ the norm operations.

Then the core of frequency domain multiquadric interpolation is to determine coefficients $\alpha_i(k)$. In order to determine them, we must solve a set of linear equations. Its matrix form is as follows:

$$Z = Q_r \alpha \tag{7}$$

where $Q_r$ is the radial basis function matrix, $\alpha$ the weighted factor matrix, $Z$ the current scan echo matrix, with the following parameters:

$$Q_r = \begin{bmatrix} Q(R_1 - R_1),\ Q(R_1 - R_2),\ ...,\ Q(R_1 - R_i) \\ Q(R_2 - R_1),\ Q(R_2 - R_2),\ ...,\ Q(R_2 - R_i) \\ ..... \\ Q(R_i - R_1),\ Q(R_i - R_2),\ ...,\ Q(R_i - R_i) \end{bmatrix} \tag{8}$$

$$\alpha = \begin{bmatrix} \alpha_1(1),\ \alpha_1(2),\ \alpha_1(3),...,\ \alpha_1(k) \\ \alpha_2(1),\ \alpha_2(2),\ \alpha_2(3),...,\ \alpha_2(k) \\ ..... \\ \alpha_i(1),\ \alpha_i(2),\ \alpha_i(3),...,\ \alpha_i(k) \end{bmatrix} \quad Z = \begin{bmatrix} X_1(1),\ X_1(2),\ ...,\ X_1(k) \\ X_2(1),\ X_2(2),\ ...,\ X_2(k) \\ ..... \\ X_i(1),\ X_i(2),\ ...,\ X_i(k) \end{bmatrix} \tag{9}$$

In Equation (9), $X_i(k)$ is the current scan echo signal in the $k$th pulse of the $i$th selected range bin. So we can solve for $\alpha$:

$$\alpha = Q_r^{-1} Z \tag{10}$$

By substituting $\alpha_i(k)$ into Equation (5), the weather signal recovered by frequency domain multiquadric interpolation can be obtained.

### 3.3. Two-dimensional Joint Interpolation in Range-Doppler Domain

The improved multiquadric interpolation described in the previous section still has some drawbacks. The improved multiquadric interpolation is still one-dimensional spatial interpolation, which only explores the spatial continuity of weather data and loses the information of time dimension.

The proposed algorithm extends the improved multiquadric interpolation to the two-dimensional joint interpolation in range-Doppler domain. After calculating the weather signal restored by one-dimensional interpolation in range domain, the weather signal restored by one-dimensional interpolation in Doppler domain is calculated. Finally, two dimension joint interpolation is carried out according to the two dimension coefficients calculated by the least square method. The specific steps of the proposed algorithm are as follows:

1) Calculate the cross-covariance matrix over the selected range bins with current and previous scans, and it has the expression:

$$\hat{R} = \frac{1}{N} Z_0^T Z \tag{11}$$

with the following matrix:

$$Z_0 = \begin{bmatrix} X_1^0(1),\ X_1^0(2),\ ...,\ X_1^0(k) \\ X_2^0(1),\ X_2^0(2),\ ...,\ X_2^0(k) \\ ..... \\ X_i^0(1),\ X_i^0(2),\ ...,\ X_i^0(k) \end{bmatrix} \quad i = 1, 2, ..., N \tag{12}$$

where $X_i^0(k)$ is the previous scan echo signal in the $k$th pulse of the $i$th selected range bin, $N$ the total number of range bins selected, and $[\cdot]^T$ the operations of transposition.

2) Calculate the first moment of the cross-covariance matrix, denoted as:

$$o = E[\hat{R}] \tag{13}$$

3) According to the first moment of the cross-covariance matrix calculated in 2), the previous scan echo signal of the weather radar is translated. The weather signal recovered by one-dimensional interpolation in Doppler domain in the $k$th Doppler bin can be written as:

$$\hat{\hat{X}}_l(k) = \frac{1}{N} \sum_{i=1}^{N} (X_i^0(k) + o(k)), \quad k = 1, 2, ..., K \tag{14}$$

4) Compute the two-dimensional weighted coefficients by completing a least mean squares analysis on the weather signal recovered by one-dimensional interpolation in Doppler domain, the weather signal recovered by improved multiquadric interpolation, and known values for the selected range bins.

5) Utilize the two-dimensional weighted coefficients to combine the weather signal recovered by one-dimensional interpolation in Doppler domain and the weather signal recovered by improved multiquadric interpolation.

The following equation describes how the weather signal recovered by improved multiquadric interpolation $(\hat{X}_l(1), \hat{X}_l(2), ..., \hat{X}_l(k))$ is combined with the weather signal recovered by one-dimensional interpolation in Doppler domain $(\hat{\hat{X}}_l(1), \hat{\hat{X}}_l(2), ..., \hat{\hat{X}}_l(k))$ to form a single estimate vector $Y$.

$Y$ is given by:

$$Y = \varpi^T \begin{bmatrix} \hat{X}_l(1),\ \hat{X}_l(2),\ ...,\ \hat{X}_l(k) \\ \hat{\hat{X}}_l(1),\ \hat{\hat{X}}_l(2),\ ...,\ \hat{\hat{X}}_l(k) \end{bmatrix} \tag{15}$$

where $\varpi$ is the two-dimensional weighted coefficients, and the above formula can be written in matrix form:

$$Y = \varpi^T P \tag{16}$$

where $P = \begin{bmatrix} \hat{X}_l(1),\ \hat{X}_l(2),\ ...,\ \hat{X}_l(k) \\ \hat{\hat{X}}_l(1),\ \hat{\hat{X}}_l(2),\ ...,\ \hat{\hat{X}}_l(k) \end{bmatrix}$, the residual sum of squares function $D$ is introduced:

$$D(\varpi) = \|Y - P_z\|^2 = \|\varpi^T P - P_z\|^2 \tag{17}$$

where $P_z = [\frac{1}{N}\sum_{i=1}^{N} X_i(1),\ \frac{1}{N}\sum_{i=1}^{N} X_i(2),\ ...,\ \frac{1}{N}\sum_{i=1}^{N} X_i(k)]$.

In order to make the interpolation accuracy as high as possible and realize the accurate recovery of the weather signal, it can be known from the least mean squares criterion that $D(\varpi)$ should be made as small as possible.

When $\varpi = \hat{\varpi}$, $D(\varpi)$ is the minimum, denoted as:

$$\hat{\varpi} = \arg\min(D(\varpi)) \tag{18}$$

By finding the minimum value of $D(\varpi)$, the following equation can be obtained:

$$PP^T\hat{\varpi} = PP_z^T \tag{19}$$

Therefore, $\hat{\varpi}$ can be solved

$$\hat{\varpi} = (PP^T)^{-1}PP_z^T \tag{20}$$

## 4. SIMULATION RESULTS AND PERFORMANCE ANALYSES

The validity of the proposed algorithm is verified by computer simulation. The main simulation parameters of the radar system are listed in Table 1 [15]. We select the 25th range bin as the range bin contaminated by WTC and select the 23th, 24th, 26th, 27th range bins as interpolation samples.

For the sake of simplicity, the mean absolute error (MAE) in radial velocity estimation is adopted to evaluate the interpolation performance. We compare the radial velocity estimation before and after applying the interpolation algorithm. MAE and mean values of radial velocity estimation for each interpolation algorithm are calculated respectively. In order to make the experimental results more accurate, we conduct 100 independent Monte Carlo experiments.

**Table 1.** Main simulation parameters.

| Parameters | Value |
|---|---|
| Pulse Repetition Frequency (PRF) | 1000 Hz |
| Transmitted Frequency | 5.5 GHz |
| Pulses Number | 128 |
| Radar Height | 1000 m |
| Range Bins Number | 50 |
| Elements Number | 8 |

### 4.1. Radial Velocity Estimation

In the weather radar, the radial velocity estimation of the weather signal can be obtained from the following equation:

$$\hat{V} = \left(\frac{\lambda}{4\pi T_r}\right) \angle \hat{R}(1) \tag{21}$$

where $T_r$ is the pulse repetition interval, $\angle \hat{R}(1)$ the phase of lag 1 estimate of $\hat{R}(1)$, and $\hat{R}(1)$ the first-order autocorrelation parameter of the radar return, which is defined as:

$$\hat{R}(1) = \frac{1}{K-1} \sum_{n=1}^{K-1} x^*(n)x(n+1) \tag{22}$$

where $x(n)$ is the radar return in the $n$th pulse, and the symbol $*$ denotes the conjugate.

The values presented in Table 2 are obtained by calculating the MAE between the radial velocity estimation of the 25th range bin and the truth value. As we can see from Table 2, the MAE is about 4 m/s, indicating that the 25th range bin has been contaminated by WTC, and it is impossible to estimate the radial velocity of the weather signal directly from this range bin.

**Table 2.** MAE in radial velocity estimation of the 25th range bin.

| SNR/dB | −3 | −2 | −1 | 0 | 1 | 2 | 3 | 4 | 5 |
|---|---|---|---|---|---|---|---|---|---|
| MAE/(m/s) | 4.153 | 4.188 | 4.171 | 4.187 | 4.182 | 4.142 | 4.179 | 4.184 | 4.177 |

MAEs in radial velocity estimation in different SNRs are plotted in Fig. 3. When SNR is −5 dB, compared with the conventional multiquadric interpolation, the MAE of the proposed algorithm is reduced by 3.7 m/s. Compared with the improved multiquadric interpolation, the MAE of the proposed algorithm is reduced by 0.1 m/s. We choose the SNR from −5 dB to 10 dB to analyze its influence on interpolation performance. It can be seen that the MAE decreases with the increase of SNR. We notice that as a function of SNR, the MAE curve of two-dimensional joint interpolation in range-Doppler domain tends to be more stable, which shows that the proposed algorithm can effectively reduce the noise disturbance.

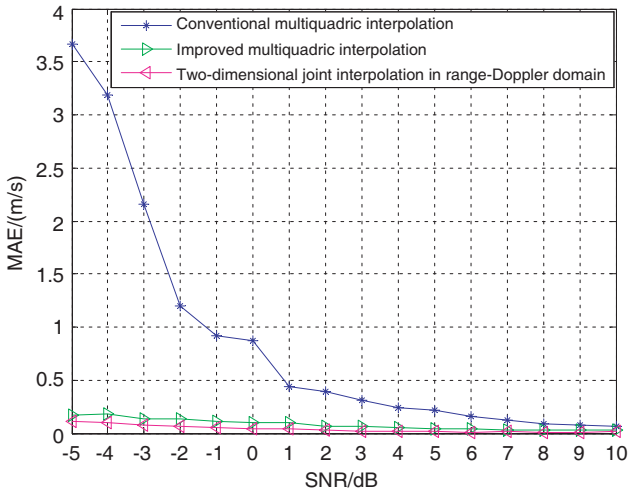


**Figure 3.** MAEs in radial velocity estimation in different SNRs.

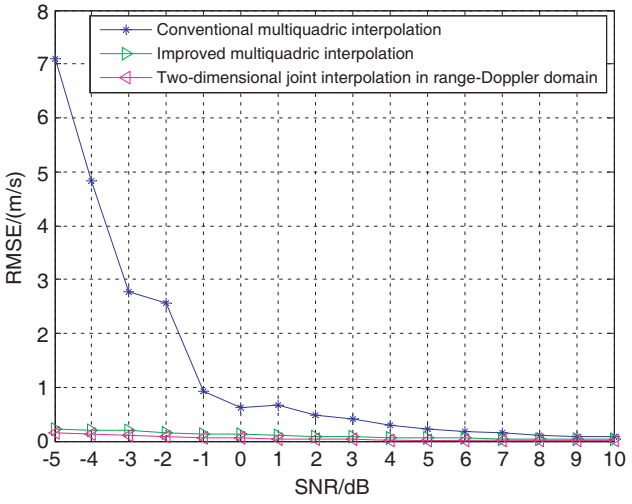


**Figure 4.** RMSEs in radial velocity estimation in different SNRs.

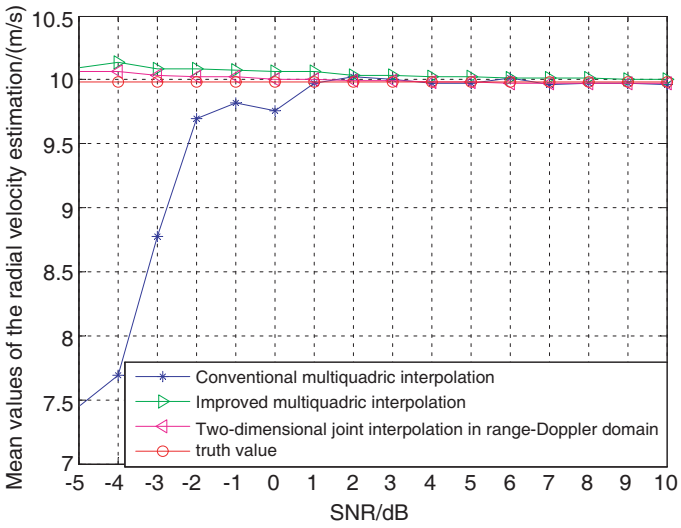


**Figure 5.** Mean values of radial velocity estimation in different SNRs.

RMSEs in radial velocity estimation in different SNRs are plotted in Fig. 4. As we can see, RMSE of the proposed algorithm has been greatly reduced, indicating that the weather signal data recovered by the proposed algorithm in this paper are the most stable with the smallest error.

Figure 5 shows the mean values of radial velocity estimation in different SNRs. In Fig. 5, the red line represents the true value of radial velocity of the weather signal, and the blue line, green line, and purple line respectively represent the mean value of radial velocity estimation of the weather signal restored by conventional multiquadric interpolation, improved multiquadric interpolation, and two-dimensional joint interpolation from 100 independent Monte Carlo experiments. From Fig. 5, we note that the mean value of radial velocity estimation of the conventional multiquadric interpolation is greatly sensitive to noise, and it is impossible to estimate the radial velocity of the weather signal in low SNR. When SNR is $-5$ dB, compared with the conventional multiquadric interpolation, the mean value of radial velocity estimation of the proposed algorithm is increased by 2.9 m/s. Compared with the improved multiquadric interpolation, the mean value of radial velocity estimation of the proposed algorithm is reduced by 0.1 m/s. As a function of SNR, the mean value of radial velocity estimation of the proposed algorithm is closer to the truth value and finally converges to the truth value.

In the case of low SNR, it is clear that the two-dimensional joint interpolation in range-Doppler domain outperforms both the conventional multiquadric interpolation and the improved multiquadric interpolation.

Finally, Fig. 6 and Fig. 7 show the range-Doppler spectrum before and after applying the two-dimensional joint interpolation, respectively. It is clear that the WTC of the 25th range bin is well suppressed.

### 4.2. Computational Complexity Analysis

Due to the ineffectiveness of the conventional multiquadric interpolation in the case of low SNR, it is meaningless to analyze its computational complexity. So we compare computational complexity of the improved multiquadric interpolation and the two-dimensional joint interpolation in range-Doppler domain. The computational complexity of the improved multiquadric interpolation is $O((N^2+N_fN)n)$, while the two-dimensional joint interpolation in range-Doppler domain is $O(N(N_f+K)n)$. Under the simulation parameters, the number of selected range bins is $N=4$, and the selected Doppler frequency bins is $N_f=22$. In addition, the number of experiments is $n=100$. Calculation results show that computational complexity of the two-dimensional joint interpolation in range-Doppler domain is greatly reduced compared with the improved multiquadric interpolation, which confirms that the proposed algorithm is suitable for engineering application.

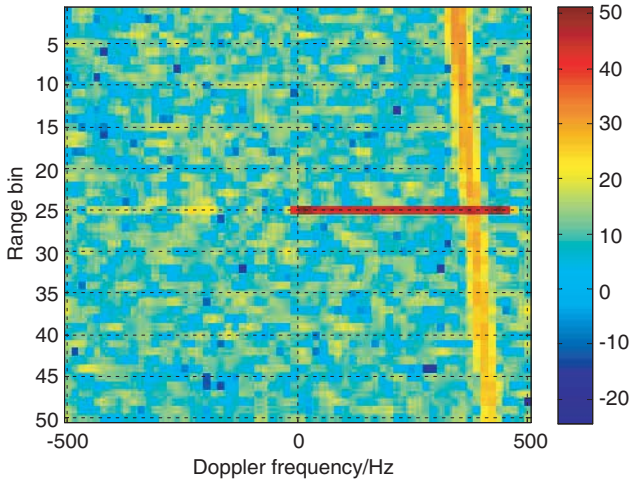


**Figure 6.** The contaminated range-Doppler spectrum.

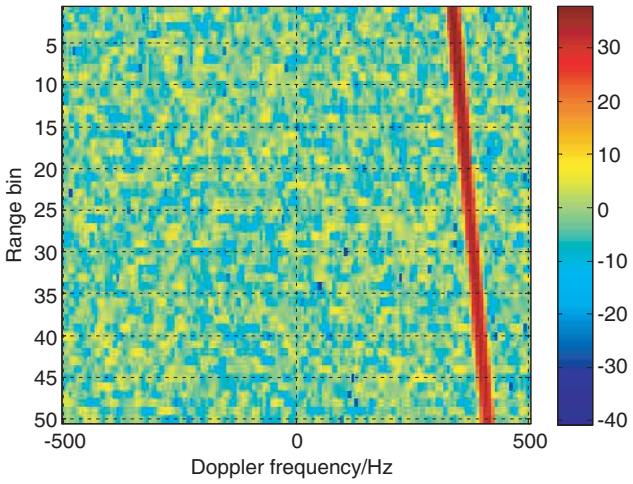


**Figure 7.** The range-Doppler spectrum after applying two-dimensional joint interpolation.

## 5. CONCLUSIONS AND FUTURE WORK

This paper proposes the two-dimensional joint interpolation in range-Doppler domain for suppression of WTC for weather radars. Firstly, the frequency-domain transformation technique is explored to overcome the problem that the interpolation algorithm cannot recover the weather signal in the case of low SNR. Then, combining spatial and spectral characteristics of the weather data, the proposed algorithm extends one-dimensional spatial interpolation to two-dimensional joint interpolation in range-Doppler domain. Simulation results illustrate that the proposed algorithm can effectively suppress the wind turbine clutter and reduce the bias in radial velocity estimation caused by WTC contamination in low SNR environments. In addition, this scheme has small computation, and it is suitable for the practical use.

The algorithm proposed in this paper is based on the spatial continuity of weather data. However, In our simulation, we call the range bin which is more than 10 range bins from the contaminated range bin as the range bin which is far away from it. We intend to classify weather data and estimate their spatial correlation to achieve the optimal interpolation performance. Details on such a expansion algorithm are forthcoming.

## ACKNOWLEDGMENT

This research was supported in part by the National Natural Science Foundation of China (No. 41830110, No. 61771182).

## REFERENCES

1. Gallardo-Hernando, B. and J. Munoz-Ferreras, "Wind turbine clutter observations and theoretical validation for meteorological radar applications," *IET Radar Sonar Nav.*, Vol. 5, No. 2, 111–117, 2011.
2. Isom, B. M., R. D. Palmer, G. S. Secrest, et al., "Detailed observations of wind turbine clutter with scanning weather radars," *J. Atmos. Ocean. Tech.*, Vol. 26, No. 5, 894–910, 2009.
3. Liu, Y. and J. He, "A study of ground clutter suppression with a regression filter," *International Conference on Signal Processing*, IEEE, 2007.
4. Barnes, S. L., "Comments on 'Use of multiquadric interpolation for meteorological objective analysiss,"' *Mon. Wea. Rev.*, Vol. 123, No. 7, 2255–2256, 1995.

5. Golbon-Haghighi, M. H., "Ground clutter detection for weather radar using phase fluctuation index," *IEEE Transactions on Geoscience and Remote Sensing*, Vol. 57, No. 5, 2889–2895, 2018.
6. Uysal, F. and I. Selesnick, "Mitigation of wind turbine clutter for weather radar by signal separation," *IEEE Transactions on Geoscience and Remote Sensing*, Vol. 54, No. 5, 2925–2934, 2016.
7. Gallardo-Hernando, B. and F. Perez-Martinez, "Detection and mitigation of wind turbine clutter in C-band meteorological radar," *IET Radar Sonar & Navig*, Vol. 4, No. 4, 520–527, 2010.
8. Hood, K., S. Torres, and R. Palmer, "Automatic detection of wind turbine clutter for weather radars," *J. Atmos. Ocean. Tech.*, Vol. 27, No. 11, 1868–1880, 2010.
9. Danoon, L. R. and A. K. Brown, "Modeling methodology for computing the radar cross section and Doppler signature of wind farms," *IEEE Trans. on Antennas & Propagation*, Vol. 61, No. 10, 5166–5174, 2013.
10. Lok, Y. F., A. Palevsky, and J. Wang, "Simulation of radar signal on wind turbine," *IEEE Aerospace & Electronic Systems Magazine*, Vol. 26, No. 8, 39–42, 2011.
11. Nuss, W. A. and D. W. Titley, "Use of multiquadric interpolation for meteorological objec tive analysis," *Mon. Wea. Rev.*, Vol. 122, No. 7, 1611–1631, 1994.
12. Yuan, Z., et al., "Phase difference measurement of undersampled sinusoidal signals based on coherent accumulation and DFT," *Geoscience & Remote Sensing Symposium*, IEEE, 2016.
13. Hardy, R. L., "Multiquadric equations of topography and other irregular surfaces," *J. Geophys. Res.*, Vol. 76, No. 8, 1905–1911, 1971.
14. Franke, R., "Scattered data interpolation: Tests of some methods.," *Math. Comput.*, Vol. 38, No. 157, 181–200, 1982.
15. Vidal, L. and W. Stephen, "C-band dual-polarization radar observation of a massive volcanic eruption in South America," *IEEE J. Sel. Topic Appl. Earth Observ.*, Vol. 10, No. 3, 960–974, 2017.